

The Recent Droughts of 2019/20 in Southern Africa and Its Teleconnection with ENSO Events

Berhanu F. Alemaw

Department of Geology, University of Botswana, Gaborone, Botswana
Email: alemaw@ub.ac.bw, bfailemaw@gmail.com

How to cite this paper: Alemaw, B.F. (2022) The Recent Droughts of 2019/20 in Southern Africa and Its Teleconnection with ENSO Events. *Atmospheric and Climate Sciences*, 12, 246-263.

<https://doi.org/10.4236/acs.2022.122015>

Received: December 7, 2021

Accepted: March 11, 2022

Published: March 14, 2022

Copyright © 2022 by author(s) and Scientific Research Publishing Inc. This work is licensed under the Creative Commons Attribution International License (CC BY 4.0).

<http://creativecommons.org/licenses/by/4.0/>



Open Access

Abstract

This study is motivated to highlight the variability of recent drought hotspots in the region of southern Africa in terms of the seasonal and annual rainfall regimes and their possible spatial linkage with the 1950-2020 seasonal El Niño/Southern Oscillation (ENSO). Some evidence is found on possible links between the occurrence of drought hotspots in the region in terms of seasonal and mean annual runoff and warm ENSO events. This was revealed by the existence of a strong and nearly-strong positive linear correlation between Seasonal and annual rainfall depths and the warm seasonal ENSO indices explained by the southern oscillation index represented by the sea level pressure (SLP) anomalies data obtained from the National Oceanographic and Aeronautics Administration (NOAA). Considering the entire southern African region, 41% of the surface areas exhibit moderate ($r > 0.25$) and strong ($r > 0.5$) correlation coefficients in terms of the December to February quarter rainfall and ENSO indices. Above 50% confidence interval in the correlation between seasonal rainfall and ENSO during DJF quarters is found in 74% of the surface area of the region of southern Africa. The high confidence interval of the positive correlation coefficients is an indication that substantial variance of precipitation during ENSO years is accounted for by the warm ENSO events. The areas with pronounced lower rainfalls and droughts associated with ENSO activity in the region include larger and some pockets of various countries in southern Africa, including but not limited to Angola, Botswana, Lesotho, Namibia, Zambia, Zimbabwe, South Africa and Mozambique. The recent drought events of 2019/2020, and previously in 2015/16 in this region with wider regional impacts can be explained by the ENSO phenomena.

Keywords

Rainfall Variability, Drought, ENSO Episode, Correlation Analysis, Southern Africa

1. Introduction

ENSO events dramatically alter oceanic conditions, climate and weather patterns across the globe and significant correlations between large-scale regional precipitation patterns and ENSO episodes have been identified for several specific regions around the world (e.g., [1]-[6]). On a seasonal time-scale, the ENSO phenomenon affects the atmospheric circulation outside the tropics [7] [8]. South-eastern Africa tends to experience dry conditions during warm ENSO events [2] [6]. ENSO is an atmospheric phenomenon that has long been known to have a characteristic manifestation in Southern Africa whereby warm-phase episodes are associated with droughts while cold-phase episodes lead to wetter than normal conditions. Mechanisms linking above-normal sea-surface temperature (SST) anomalies over the central Indian Ocean with Southern African droughts have also been explored by Jury and Pathack [9] [10]; Landman [11]; Jury *et al.*, [12]; Tennant [13]; Landman and Klopper [14]; Rautenbach [15].

The easterly and westerly shifts of ENSO activity in the Walker circulation induce warming and cooling in remote ocean basins such as the Indian Ocean and the tropical north Atlantic, with a time lag of one to two seasons [16], with ENSO events recurring in periodical patterns. ENSO can also affect regions outside the tropics, via large-scale atmospheric waves [17]. The influence of ENSO events is profoundly felt outside the tropics as well including southern Africa as noted in recent literature on evolution of southern African summer precipitation as noted by Monerie *et al.* [18] Hoell *et al.* [19] [20]; on ENSO teleconnections e.g. Jury [2], Archer *et al.* [21] Winsemius *et al.* [22] Alemaw & Chaoka [23] and seasonal rainfall predictions as noted by Rautenbach [15] Landman & Klopper [14].

The ENSO phenomenon is one of the biggest players in the game of year-to-year climatic variability. As many researchers have now come to appreciate, these two phenomena typically occur in conjunction, about once every few years. A predictive model for the December to March rainfall season simulation for South Africa that considers ENSO influence in a canonical correlation analysis is provided by [14] Landman and Klopper (1998). Due to the heterogeneous nature of rainfall, a large number of measurement stations are required for accurate characterization of rainfall patterns over large areas. Furthermore, understanding large-scale global atmospheric dynamics will enhance our understanding of regional and local systems of rainfall occurrence, which could improve understanding of precipitation characteristics. Moreover, tropical and extra-tropical atmospheric teleconnections of ENSO have an influence on extreme hydrological phenomena such as the intensity and occurrence of extreme events such as storms, heatwaves, droughts and floods as noted by Yeh *et al.* [24] and Cai *et al.* [16].

Effect of ENSO on rainfall over large areas can be felt as integrators of river systems and the ability to predict flow patterns in rivers will be highly enhanced if the relationship between precipitation and ENSO is predicted (Alemaw and Chaoka) [23]. In earlier studies, an attempt was made to establish the relation-

ship between ENSO and the natural variability in the flow of tropical rivers such as Amazon, Congo, Parana and Nile Rivers as noted [25]. These authors reported the existence of a stronger correlation between the seasonal and annual precipitations of these rivers and seasonal ENSO indices.

A prevalence of below-normal rainfall occurrences in several regions of South Africa during El Niño years has been reported (e.g. [14] [15]). Recent studies indicate that ENSO events can be accurately predicted one to two years in advance using a physical model of the coupled ocean-atmospheric system [26], and lately in Atmosphere-Ocean General Circulation Models (AOGCM) under the Climate Model Inter-comparison Project, phase 5 (CMIP5) [1] [27].

Therefore, the motivation of this paper is to explore whether a relationship exists between precipitation and ENSO and to quantify the relationship in the Southern African rainfall drought regimes that occurred during ENSO events. Emphasis is given to the drier ENSO events to examine the possible link with the decline in rainfall regimes in this region in the recent drought period of 2019/20 and those between 2005 and 2019/20.

In this paper, the relationship between seasonal quarter warm ENSO events in terms of the SLP anomalies data and 1 degree resolution precipitation data of southern Africa has been retrieved from the global gridded data base of the Global Precipitation Climatology Centre (GPCC) [28]. The monthly datasets were converted to seasonal and annual ensembles for each 1deg grid covering the region of southern Africa. The seasonal ensembles were the quarterly ENSO indices of the three-month aggregate mean values of December to February (DJF), March to May (MAM), June to August (JJA) and September to November (SON).

The global gridded precipitation datasets are produced by methods developed to produce real-time rain gauge-satellite merged analyses of global monthly precipitation as noted in [29]. The datasets contain global monthly precipitation analyses that are composed of a mix of rain gauge observations and satellite estimates. These are based on the Global Precipitation Climatology Project (GPCP) combined analysis products described by [29] and the Climate Prediction Center Merged Analysis of Precipitation (CMAP) presented in [30].

The objective of this manuscript is to document results of correlation and spatial analysis specifically aimed at investigating the type and magnitude of possible correlations between warm ENSO activity and the regional implications of the seasonal and annual precipitation over the southern African region. Possible explanations are also presented for the possible link between the long-term ENSO patterns and trends in annual precipitation pattern and the spatial coherence of the ENSO-precipitation correlation over the region explained in terms of confidence interval of the prevailing rainfall-ENSO correlation coefficients.

2. Data Used

Gridded datasets at a spatial scale of 1 degree were extracted for the region of southern Africa from global database of the Global Precipitation Climatology Centre (GPCC) [28]. The GPCC dataset from 2005 to February 2020 was ex-

tracted to investigate the teleconnection between the rainfall in the region of southern Africa and the most recent ENSO activity that occurred from early 1950s to date. The annual precipitation of the study region for 2019/2020, re-sampled from the GPCC dataset using the nearest neighborhood method is presented in **Figure 1**.

To assess the effect of ENSO phenomenon on the rainfall regime of the region with the concurrent period of the ENSO data available from NOAA that extends as early as 1951 (**Figure 2**), rain-gauge data for stations nearby selected grid points

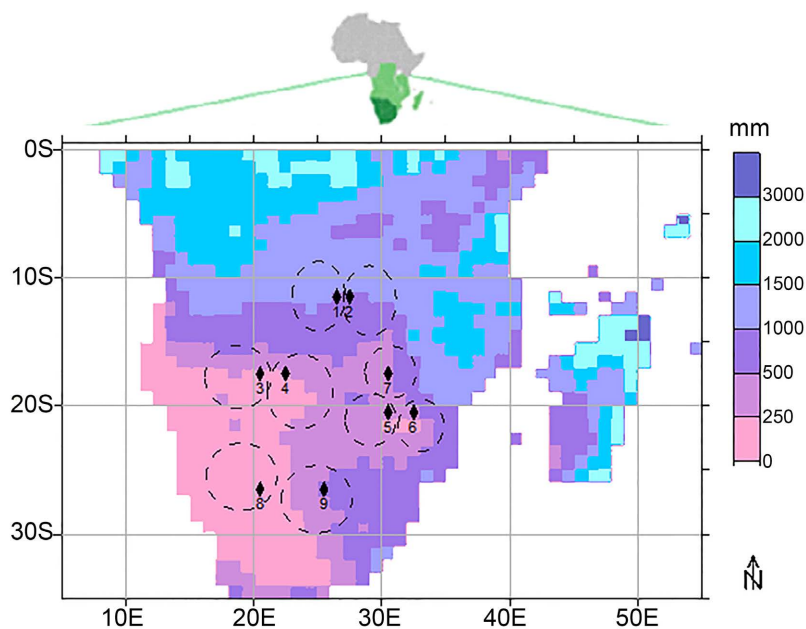


Figure 1. Southern Africa variation of 2019/2020 Annual Rainfall and selected rainfall Stations from FRIEND data base. Data source: [31].

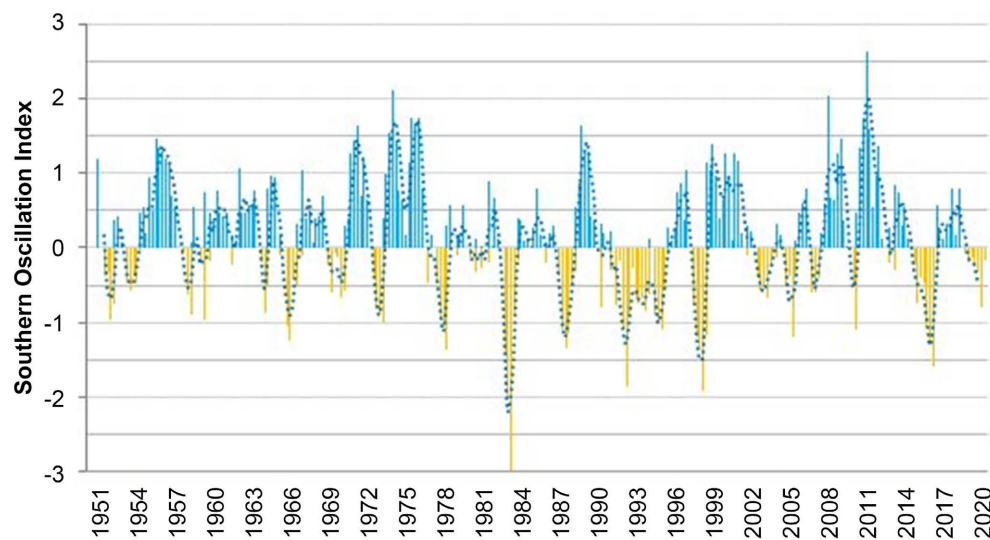


Figure 2. Time series plots of aggregated 3-month ENSO mean sea-level pressure (SLP) anomalies (solid bars) and three month moving averages (dashed lines) for January 1951 to February 2020. Data source: [32].

in the region are also further explored. The Flow Regimes from International Experiments and Network Data (FRIEND) data stations are also shown in **Figure 1**. Precipitation time series data of nine gauging stations from southern African countries were acquired from the database of FRIEND Project coordinated at the University of Dar es Salaam [31]. Quality of daily and monthly precipitation discharge data was checked and then annual precipitation time series data was extracted to complement the GPCC gridded dataset rainfall data of the study region. Details of the rainfall data used are summarized in **Table 1**.

Even though the period of available record is not sufficiently long enough, the authors thrust that the data set is fairly sufficient to draw some conclusions regarding spatial variability of precipitation in the region and its possible correlation with ENSO phenomena. It is also fairly speculated that the data can be used to build on the similar studies conducted in the regional focusing to some extent on few countries and sub-regions of the region of southern Africa.

Monthly dataset of SLP anomalies are acquired from database of the NOAA and are acquired from the Climate Prediction Centre (CPC) official web site [32]. **Figure 2** depicts the monthly mean Southern Oscillation Index in terms of sea-level pressure (SLP) anomalies expressed in standard units for the period from January 1951 to February 2020 expressed in standard units, which is a measure of the pressure difference between the central (Tahiti) and western Pacific (Darwin).

Coincident periods for both ENSO events and precipitation were selected and analyzed. Of the 24 El Niño events that have occurred in the century just ended, about 13 of the strongest historical El Niño events have occurred between 1950s and early 2000s, as documented by different authors for the various periods [7] and six additional ENSO events have occurred between 2000 and 2001/9/20. The prominent ENSO/El-Niño years are from December to January of 1951/52, 1953/54, 1957/58, 1963/64, 1965/66, 1969/70, 1972/73, 1977/78, 1982/83, 1987/88, 1991/92, 1994/95, 1997/98, 2002/03, 2004/05, 2006/07, 2009/10, 2015/16 and 2019/20.

Table 1. Details of data used in the study.

| Station ID | Degree Longitude | Degree Latitude | Locality of Grid Center | FRIEND Time Series Database | GPCC Gridded Data set |
|------------|------------------|-----------------|------------------------------------|-----------------------------|-----------------------|
| 1 | -11.5 | 26.5 | North Zambia/Southern DRC | 1961-96 | 2005-19 |
| 2 | -11.5 | 27.5 | North Zambia/Southern DRC | 1961-97 | 2005-19 |
| 3 | -17.5 | 20.5 | N Namibia/Southern Angola | 1950-97 | 2005-19 |
| 4 | -17.5 | 22.5 | E Namibia/W Zambia/N Botswana | 1980-96 | 2005-19 |
| 5 | -20.5 | 30.5 | Southern Zimbabwe | 1975-98 | 2005-19 |
| 6 | -20.5 | 32.5 | Eastern Zimbabwe/W Mozambique | 1960-95 | 2005-19 |
| 7 | -17.5 | 30.5 | Northern Zimbabwe | 1959-93 | 2005-19 |
| 8 | -26.5 | 20.5 | SE Namibia/W Botswana/NW S. Africa | 1961-97 | 2005-19 |
| 9 | -26.5 | 25.5 | S Botswana/Northern South Africa | 1961-98 | 2005-19 |

These El Niño years are similar to those defined by other researchers [5] [21]. The selected monthly historical ENSO periods were each split into 4 consecutive three-month quarters of December to February (DJF), March to May (MAM), June to August (JJA) and September to November (SON). The main reason for creating different subsets was to better capture the influence of ENSO on the rainfall as a proxy for the occurrence and variability of precipitation in the region of southern Africa.

3. Methodology

3.1. Correlation Analysis

The methodology used in this study comprised correlation analysis of the mean annual runoff and three-month quarter warm ENSO indices during the concurrent El Niño years considered. The hydrological year or seasonal cycle defined as a 12-month period starting from the month of lowest average rainfall for each year was selected. For all the 1 degree grids covering southern Africa, the seasonal cycle of flow and the annual flow depths are determined. The type and magnitude of the correlation are also investigated. We have also attempted to explore the possible evidence of a link between the long-term ENSO patterns and trends in seasonal and annual runoff pattern across the region of Southern Africa.

The variance accounted for by El Niño in the natural variability of precipitation of selected locations in Southern Africa is established. In order to avoid possible lag correlation between seasonal precipitation and seasonal SLPs, a correlation analysis is conducted with the annual discharge, against eight quarters of SOI in terms of SLP anomalies. Eight quarters are formed from four ENSO/SOI quarters during El Niño years, and two quarters each before and after El Niño years.

We measured the association between ENSO and precipitation using the linear correlation coefficient, r (also called the product-moment correlation coefficient, or Pearson's r). In order to assess whether a correlation is significant, we use the test statistic, t , to identify the confidence level of the correlations between ENSO and the terrestrial hydro-climatological variable of precipitation. The test statistic, t , is defined by [33] as:

$$t = r \sqrt{\frac{N-2}{1-r^2}} \quad (1)$$

which is distributed in the null hypothesis case (of no correlation) like the student's t -distribution denoted by $A(t/v)$ with $v = N - 2$ degrees of freedom. $1 - A(t/v)$ is the significance level at which the hypothesis that the means are equal is disproved. The mathematical definition of the function is given by:

$$A(t/v) = \frac{1}{v^{1/2} B\left(\frac{1}{2}, \frac{v}{2}\right)} \int_{-t}^t \left(1 + \frac{x^2}{v}\right)^{-\frac{v+1}{2}} dx \quad (2)$$

with lower and upper limiting values, respectively given by:

$$A(0/v) = 0 \quad \text{and} \quad A(1/\infty) = 1 \quad (3)$$

$A(t/v)$ is related to the incomplete beta function $I_x(a; b)$ by:

$$A(t/v) = 1 - I_{\frac{v}{v+t^2}}\left(\frac{v}{2}, \frac{1}{2}\right) \quad (4)$$

The confidence level, γ for the t -statistic $t(r, v)$ is then computed as given in [34] and further noted of its application in [23] as follows:

$$\gamma(t, v) = \int_{-t(r, v)}^{t(r, v)} f(t, v) dt \quad (5)$$

3.2. Sample Size Uncertainties

Sample size uncertainties and the Pearson correlation model capabilities are investigated to determine the contribution of internal ENSO variability on the rainfall trend and drought regime in the region [33] [34]. This is particularly true when the recent period ENSO events from 2005 to early 2020 only capture about 5 cycles that relate to lower rainfall depths obtained from the corresponding period of GPCC gridded rainfall data of the region of southern Africa.

The number of samples used to quantify the linkage between ENSO and precipitation in terms of the Pearson correlation model capabilities would affect degree of robustness of the model (Figure 3) [33] [34]. By combining Equations (1) and (5), the confidence interval, $\beta = (1 - \gamma)100\%$ is computed (see Figure 3 for the sample size of 5, which is the number of datasets attributed to the warm ENSO events that occurred during the period of analysis of date set from 2005 to February 2020). A confidence level γ indicates that $(1 - \gamma)100\%$ of the variability is attributable to random variability. FORTRAN routines provided in Numerical Recipes [34] are used to compute the confidence intervals. Before applying the test, we normalised the data and also demonstrated the possible loss of power of the t -test as a result of the small sample size considered as shown in Figure 3 for

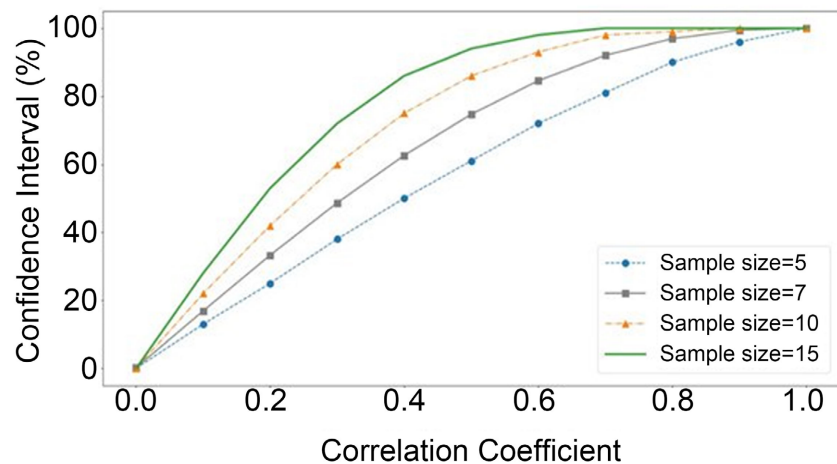


Figure 3. Relation of the correlation coefficients and the confidence intervals used in the study.

different sample sizes ranging between 5 to 15 samples. It can be noted that for correlation coefficient of 0.5 the confidence interval in the estimate of $r = 0.5$ would increase from 60% to nearly 85% as sample size increase from 5 to 15 sample sizes.

4. Results and Discussion

4.1. Correlation Coefficients and Confidence Intervals

A correlation coefficient between seasonal warm ENSO indices and annual of a typical station in western Botswana bordering SE Namibia and NW South Africa over 8 consecutive quarters is shown in **Table 2**. It shows that the mean annual precipitation is positively correlated with the four quarter ENSO periods observed during the El Niño years. Amongst the 8 quarters, a strong positive correlation ($r > 0.52$) seems to be apparent in the rainy season DJF and MAM quarters. The confidence level of the correlation coefficient for these quarters is above 95%. The positive correlation diminishes for the other seasonal quarters, and the correlation becomes negative in the quarters that precede and follow the El Niño years. For this reason, we studied the correlation between the DJF quarter warm ENSO indices and annual and concurrent seasonal precipitation of the region.

Table 2 and **Table 3** show the correlation coefficients and confidence interval between the seasonal and annual rainfall at selected sites across the Southern African region and the three-month mean warm ENSO indices of December to February (DJF). The computations were made based on two datasets that represent the period before and after 2005 over a span of early 1960s to early 2000s.

The link between seasonal rainfall in the region of Southern Africa and ENSO of December to February (DJF) in terms of Pearson correlation coefficient and

Table 2. Coefficients of cross-correlation between quarterly ENSO anomalies and mean annual precipitation during El Niño years of a station located in S Namibia and NW South Africa.

| Quarter | | Correlation. Coef. (r) | Significance level (p) | Confidence Interval (%) |
|------------------------------------|-----|----------------------------|----------------------------|-------------------------|
| June, July, August (JJA) | [-] | -0.403 | 0.113 | 88.7 |
| September, October, November (SON) | [-] | -0.260 | 0.313 | 68.7 |
| December, January, February (DJF) | [E] | 0.647 | 0.007 | 99.3 |
| March, April, May (MAM) | [E] | 0.504 | 0.047 | 95.3 |
| June, July, August (JJA) | [E] | 0.436 | 0.091 | 90.9 |
| September, October, November (SON) | [E] | -0.410 | 0.114 | 88.6 |
| December, January, February (DJF) | [+] | -0.179 | 0.492 | 50.8 |
| March, April, May (MAM) | [+] | -0.637 | 0.006 | 99.4 |

Key: [E]—El Niño year; [-]—Quarters preceding El Niño year; [+]—Quarters following El Niño year.

Table 3. Correlation coefficient and confidence intervals based on based on gridded GPCP monthly rainfall data of 2005-2020.

| Station ID | Seasonal Rainfall and ENSO during DJF quarter | | | Annual Rainfall and DJF Quarter ENSO Index | | |
|------------|---|---------------------------|-------------------------|--|---------------------------|-------------------------|
| | Cor. Coef. (r) | Significant level (p) | Confidence interval (%) | Cor. Coef. (r) | Significant level (p) | Confidence interval (%) |
| 1 | 0.869 | 0.055 | 94.5 | 0.518 | 0.371 | 62.9 |
| 2 | 0.749 | 0.145 | 85.5 | 0.328 | 0.590 | 41.0 |
| 3 | 0.235 | 0.703 | 29.7 | 0.636 | 0.249 | 75.1 |
| 4 | 0.369 | 0.541 | 45.9 | 0.740 | 0.152 | 84.8 |
| 5 | 0.200 | 0.747 | 25.3 | 0.466 | 0.429 | 57.1 |
| 6 | 0.588 | 0.298 | 70.2 | 0.587 | 0.298 | 70.2 |
| 7 | 0.758 | 0.137 | 86.3 | 0.846 | 0.071 | 92.9 |
| 8 | -0.072 | 0.909 | 9.1 | 0.397 | 0.509 | 49.1 |
| 9 | -0.859 | 0.062 | 93.8 | -0.505 | 0.385 | 61.5 |

the confidence interval is shown in **Figure 4**. The corresponding correlation coefficients and the confidence interval between annual rainfall in the region of Southern Africa and quarterly ENSO of December to February (DJF) is presented in **Figure 5**. There is a marked similarity between these two figures, which is a clear indication that DJF quarter is a rainy season whose rainfall represents substantial proportion of the annual rainfall amount in the region.

4.2. Annual and Seasonal Rainfall with ENSO Activity

Comparative investigations have been conducted to further investigate the association between annual rainfall and annual ENSO activity over annual time cycle presented in **Table 4**. It can be seen that this figure is still very much closer to the previous two figures highlighting the strong correlation between rainfall and ENSO activity, with a more pronounced effect observed during ENSO quarterly season of DJF.

Regional summary of correlation coefficients and confidence intervals of Seasonal and annual rainfall with DJF ENSO indices is provided in **Table 5**, which summarizes the correlation coefficient for the region of southern Africa in terms of percentage area distribution of the Pearson coefficient as well as confidence intervals.

4.3. Regional Rainfall and ENSO Activity

Of the entire 1 degree gridded area of southern Africa, 40.5%, 32.6% and 26.9% of the region has Pearson correlation coefficient with ranges of 0.25 to 1.0; -0.25 to 0.25 and -0.25 to -1.0 between the seasonal rainfall and ENSO during the quarters of December to February (DJF). The same corresponding correlation coefficient ranges in the region between annual rainfall and ENSO is found to be 41.2%, 33.0% and 26.0%, respectively.

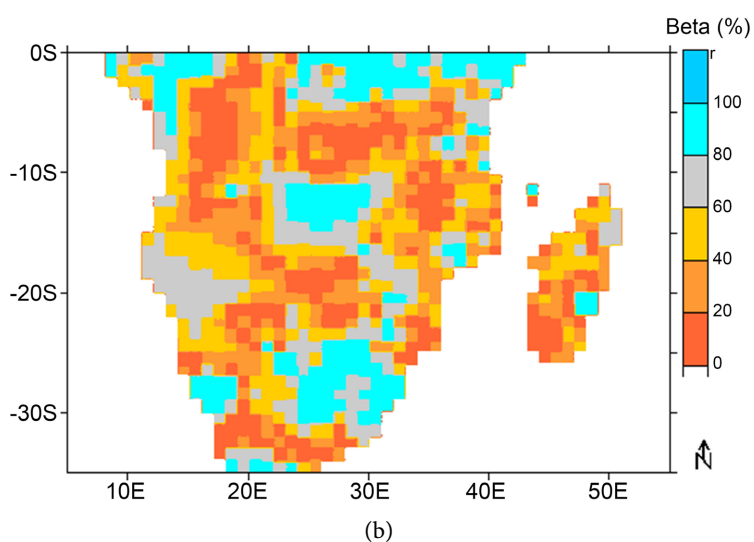
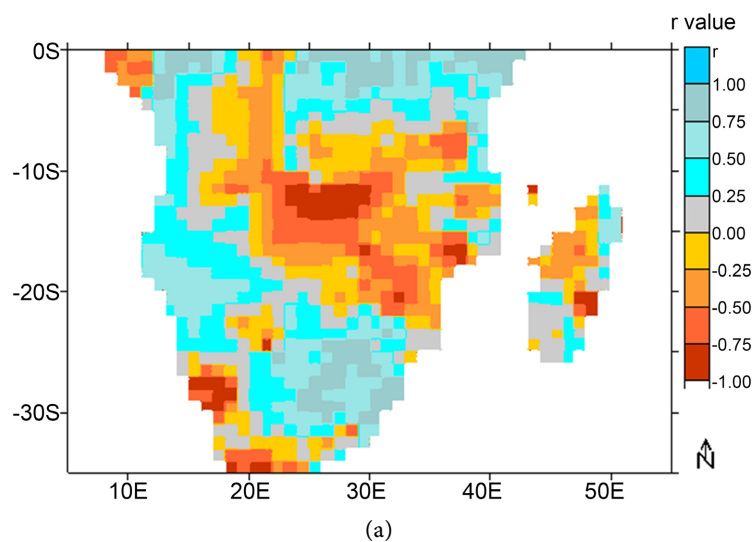
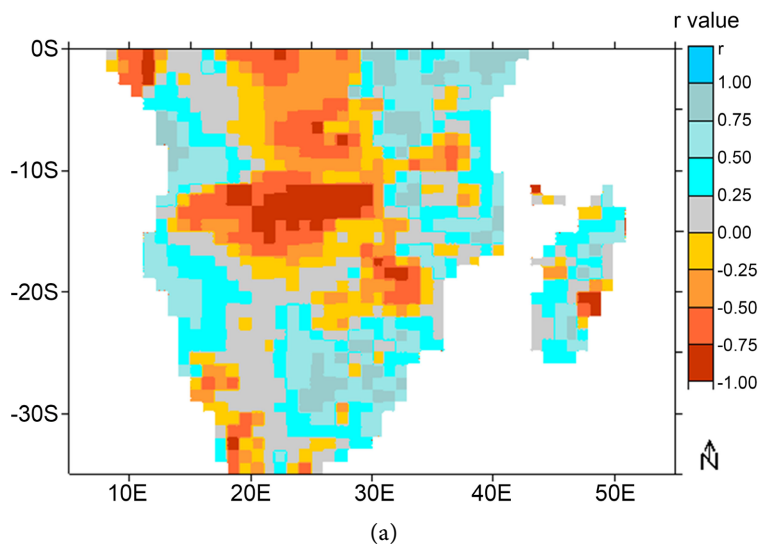


Figure 4. The link between seasonal rainfall and ENSO of December to February (DJF) in the region of Southern Africa (a) Correlation coefficient; (b) Confidence Interval in percent.



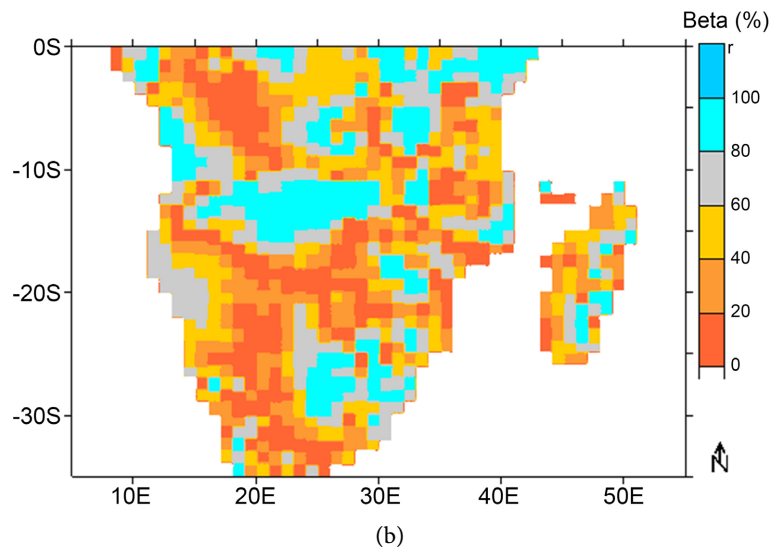


Figure 5. The link between annual rainfall and ENSO of December to February (DJF) in the region of Southern Africa (a) Correlation coefficient; (b) Confidence Interval in percent.

Table 4. Correlation coefficient and confidence intervals based on FRIEND monthly data of 1961 to early 2000s.

| Station ID | Seasonal Rainfall and ENSO during DJF quarter | | | Annual Rainfall and DJF Quarter ENSO Index | | |
|------------|---|--------------------------------|-------------------------|--|--------------------------------|-------------------------|
| | Cor. Coef. (<i>r</i>) | Significant level (<i>p</i>) | Confidence interval (%) | Cor. Coef. (<i>r</i>) | Significant level (<i>p</i>) | Confidence interval (%) |
| 1 | 0.508 | 0.037 | 96.2 | 0.114 | 0.527 | 47.3 |
| 2 | 0.544 | 0.024 | 97.5 | 0.047 | 0.816 | 18.4 |
| 3 | 0.336 | 0.187 | 81.2 | 0.089 | 0.571 | 42.9 |
| 4 | 0.122 | 0.641 | 35.9 | 0.089 | 0.762 | 23.8 |
| 5 | 0.796 | 0.001 | 99.9 | 0.427 | 0.251 | 74.9 |
| 6 | -0.051 | 0.852 | 14.7 | 0.002 | 0.993 | 0.7 |
| 7 | -0.346 | 0.189 | 81.1 | -0.021 | 0.922 | 7.8 |
| 8 | 0.647 | 0.007 | 99.3 | 0.241 | 0.183 | 81.7 |
| 9 | 0.509 | 0.044 | 95.6 | 0.491 | 0.004 | 99.6 |

Table 5. Regional summary of correlation coefficients and confidence intervals of Seasonal and annual rainfall with DJF ENSO anomaly indices.

| Seasonal Rainfall and ENSO during DJF quarter | | | Annual Rainfall and DJF Quarter ENSO indices | | |
|---|--------------------|-------|--|--------------------|-------|
| Cor. Coef. (<i>r</i>) | Proportion of area | | Cor. Coef. (<i>r</i>) | Proportion of area | |
| -1.0 to -0.50 | 12.9% | | -1.0 to -0.50 | 15.1% | |
| -0.50 to -0.25 | 14.1% | 26.9% | -0.50 to -0.25 | 10.9% | 26.0% |
| -0.25 to 0.00 | 15.1% | | -0.25 to 0.00 | 13.6% | |

Continued

| | | | | | |
|--------------|-------|-------|--------------|-------|-------|
| 0.00 to 0.25 | 17.4% | 32.6% | 0.00 to 0.25 | 19.4% | 33.0% |
| 0.25 to 0.50 | 17.5% | | 0.25 to 0.50 | 17.9% | |
| 0.50 to 1.00 | 23.0% | 40.5% | 0.50 to 1.00 | 23.3% | 41.2% |

Considering the entire southern African region, 40.5% of the surface area exhibit strong positive correlation in terms of the December to February quarter rainfall and ENSO indices, including 17.4% of the area attributed to positive but weak correlation.

The confidence interval of the correlation coefficients between seasonal rainfall ENSO anomalies during DJF quarters is 74% whereas, between annual precipitation and DJF quarter ENSO indices reaches 84%, signifying substantial variance of precipitation during ENSO years is accounted for by the warm ENSO activity.

Strong positive correlation with ENSO activity is found to cover southern Zimbabwe, area around south eastern Namibia/North Western South Africa and southern Botswana/northern South Africa as well as North Zambia/Southern DRC. Most of these areas in the region represent areas with lower rainfall regime in general with lower water security, with implications of water scarcity which were hard-hit with water shortages in 2019 and early 2020.

Occurrence of below-normal rainfall amounts from December to March during El Niño years and warm ENSO positive association with drier rainfall conditions have been noted in South Africa in several studies [2] [14] [21] [22].

In particular, the results of the regression analysis (**Figure 4**) confirm a weak yet statistically significant association between ENSO and the latitudinal position of the Angola low as noted in [35]. This also agrees with the conclusions in [35] [36], specifically for January to March season of 1998, which further supports the notion that internal atmospheric extratropical variability is partly responsible of the Angola low low-frequency variability.

4.4. Recent Drought of 2019/20

Annual rainfall variation at a station located in an area centered on grid 25.50°E/25.50°S in southern Botswana and northern South Africa is shown in **Figure 6**. It clearly shows the 2019/20 rainfall signifies very low rainfall and drought that occurred in the region. Below-average production and drought impacts are felt in larger and some pockets of various countries in southern Africa, including but not limited to Angola, Botswana, Lesotho, Namibia, Zambia, Zimbabwe, South Africa and Mozambique. The areas identified in this study with below rainfall regimes associated with warm ENSO events are similar to recent observation and model simulation of North American Multi-Model Ensemble (NMME) probabilistic forecast for precipitation for January to March 2020 based on NOAA/CPC, which is widely used for forecasting outlook assessment of drought impacts by FEWSnet [37].

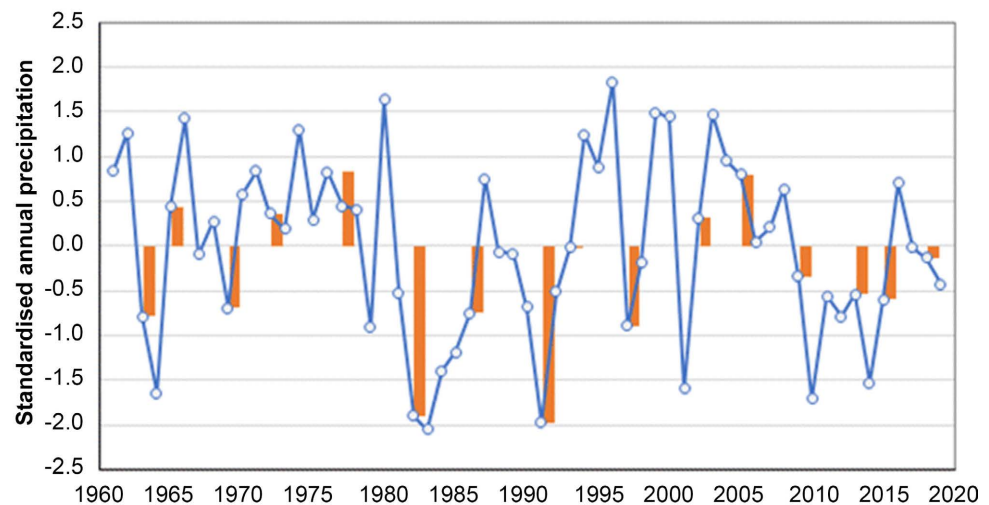


Figure 6. Annual rainfall variation showing ENSO/La Niña years at a station located in an area centered on grid 25.50°E/25.50°S in southern Botswana and northern South Africa.

A number of climate indicators are noted to have changed in the year up to end of 1990s, especially around the Pacific Basin. As can be seen on **Figure 2**, before end of 1990s El Niño seems to have occurred with about equal frequency, each at intervals of about 3 to 7 years, and between 1960 and 1990 alone, there have been about 7 El Niños (almost one every 4 years). **Figure 6** depicts standardized annual rainfall variation showing ENSO/La Niña years at a station located in an area centered on grid 25.50°E/25.50°S in southern Botswana and northern South Africa.

Below normal in the annual rainfall of 2019/20 in southern Africa, calculated from global gridded data base of the Global Precipitation Climatology Centre (GPCC) provided by Ziese *et al.* [28] is depicted in **Figure 1**. Below normal rainfall are recorded in southern Africa and higher rainfalls are recorded in equatorial parts of Southern Africa especially in the Congo River basin.

This analysis of the long-term trend of the El Niño phenomenon over the period 1950 to early 2020, depicted in **Figure 2** and **Figure 6**, supports the findings of decline in precipitation in Southern Africa shown in **Table 4** and **Figures 4-6** and corroborated in other studies, e.g. [1] [19] [20] [38] [39].

The studies demonstrate the occurrence of low seasonal rainfall totals together with high seasonal temperatures during preceding seasons of El Niño/ENSO years are likely to be more frequent under future climate change as noted in Archer *et al.* [21] and [22]. Also the studies and the reported results also highlight the potential importance of the ENSO activity for southern African rainfall [36] [40] [41] [42]. ENSO events are also found to be an important phenomenon in modulating the skills of regional climate and CMIP5 models as illustrated by Dieppois *et al.* [1] and Taylor *et al.* [27].

Recent studies by Monerie *et al.* [18], Archer *et al.* [21] and Winsemius *et al.* [22] corroborate occurrence of low seasonal rainfall totals together with high seasonal temperatures during preceding seasons during El Niño/ENSO years are

likely to be more frequent under future climate change.

Predicting climate for future seasons to several decades is useful for decision makers to adapt policies to near-term climate change [43]. The effect of low precipitations would be a potential revelation for decline of runoff of some rivers in southern Africa which would determine water resources availability for societal demands as noted by Alemaw and Chaoka [23].

The need to anticipate damages due to climate variability is a stressful problem, especially in developing countries, which are more vulnerable to climate hazards. Climate projections are mostly provided by simulations performed with Atmosphere-Ocean General Circulation Models (AOGCM) under the Climate Model Intercomparison Project, phase 5 (CMIP5) [1] [18] [27].

The ability of CMIP5 models to simulate realistic summer rainfall variability of rainfall over southern African and noted the summer teleconnections with global SSTs from extended reconstructed SST version 4 (ERSST.v4) dataset of the National Climatic Data Centre is examined by Dieppois *et al.* [1]. The modelling study through various models demonstrated the impact of SST variability in the South Atlantic and South Indian Oceans on rainfall variability in southern Africa. With various degrees of association between SST and SA rainfall is also reported and documented for different time scales and time horizons.

These precipitation forecast products have been applied for forecasting and operational applications including the following: climate modelling [1] [21] [41]; precipitation extremes [38]; and regional agriculture and vulnerability assessment [37] [44]. Other applications also include rainfall and river flow analysis [5] [23]; real-time precipitation monitoring [43] [45]; fisheries and aquaculture [17]; and study of greenhouse gas forcing [24].

All together these results also corroborate the potential importance of the ENSO activity for southern African rainfall, as suggested in earlier studies in the region including [36] Nicholson and Kim [36], and others [19] [20] [38] [39] [40] [41] [42]; and ENSO events in modulating the skills of CMIP5 models reported by Dieppois *et al.* [1] and Taylor *et al.* [27].

5. Conclusions

This study revealed that a strong positive correlation exists between the 1951-2019/20 warm ENSO events (explained by the Southern Oscillation Index or Sea Level Pressure anomalies) and the annual and seasonal rainfall in the Southern African region. We have also found during the El Niño years that a significant variance of the annual flow regime is accounted for by the El Niño phenomenon. The correlation is moderately and strong positive strong ($r > 0.25$) in 41% of the surface area of the region during the rainy season of December to February (DJF).

Above 50% confidence interval in the correlation between seasonal rainfall and ENSO during DJF quarters is found in 74% of the surface area of the region and that of the annual rainfall and seasonal ENSO during DJF quarters is found

in 84% of the surface area of the region of southern Africa.

It signifies the possible year-to-year variability of seasonal and annual precipitation during ENSO years is accounted for by the ENSO phenomena. More specifically, the recent droughts of 2015/16 and 2019/20 can be attributed to the ENSO activity.

Furthermore, the occurrence of low seasonal rainfall totals together with high seasonal temperatures during preceding seasons during El Niño/ENSO years are likely to be more frequent under future climate change as noted in recent literature.

Acknowledgements

The author thanks NOAA for the ENSO time series data, as well as Global Precipitation Climatology Centre (GPCC) for providing the gridded 1 Degree data covering the period of study used in the study. The author also thanks the coordinating Centre for the Southern Africa FRIEND Project based at the University of Dar es Salaam, Tanzania for providing daily rainfall data of Southern African stations used in this study as well previous data use in the 1990s for undertaking the PhD research of the author. The author also appreciates the constructive comments and suggestions of the anonymous reviewers of earlier versions of this paper.

Conflicts of Interest

The author declares no conflicts of interest regarding the publication of this paper.

References

- [1] Dieppois, B., Pohl, B., Crétat, J., Eden, J., Sidibe, M., New, M., Rouault, M. and Lawler, D. (2015) Southern African Summer-Rainfall Variability, and Its Teleconnections, on Interannual to Interdecadal Timescales in CMIP5 Models. *Climate Dynamics*, **45**, 2425-2442. <https://doi.org/10.1007/s00382-015-2480-x>
- [2] Jury, M.R. (2014) Factors Contributing to a Decadal Oscillation in South African Rainfall. *Theoretical and Applied Climatology*, **120**, 227-237. <https://doi.org/10.1007/s00704-014-1165-4>
- [3] McPhaden, M.J. (2012) A 21st Century Shift in the Relationship between ENSO SST and Warm Water Volume Anomalies. *Geophysical Research Letters*, **39**, 9706. <https://doi.org/10.1029/2012GL051826>
- [4] McPhaden, M.J., Zebiak, S.E. and Glantz, M.H. (2006) ENSO as an Integrating Concept in Earth Science. *Science*, **314**, 1740-1745. <https://doi.org/10.1126/science.1132588>
- [5] Chiew, F.H.S., Piechota, T.C., Dracup, J.A. and McMahon, T.A. (1998) El Niño/Southern Oscillation and Australian Rainfall, Streamflow, and Drought: Links and Potential for Forecasting. *Journal of Hydrology*, **204**, 138-149. [https://doi.org/10.1016/S0022-1694\(97\)00121-2](https://doi.org/10.1016/S0022-1694(97)00121-2)
- [6] Ropelewski, C.F. and Halpert, M.S. (1987) Global and Regional Scale Precipitation Patterns Associated with the El Niño/Southern Oscillation. *Monthly Weather Re-*

- view, **115**, 1606-1626.
[https://doi.org/10.1175/1520-0493\(1987\)115<1606:GARSPP>2.0.CO;2](https://doi.org/10.1175/1520-0493(1987)115<1606:GARSPP>2.0.CO;2)
- [7] Zhang, Y., Wallace, J.M. and Battisti, D.S. (1997) ENSO-Like Inter-Decadal Variability: 1900-93. *Journal of Climate*, **10**, 1004-1020.
[https://doi.org/10.1175/1520-0442\(1997\)010<1004:ELIV>2.0.CO;2](https://doi.org/10.1175/1520-0442(1997)010<1004:ELIV>2.0.CO;2)
- [8] Philander, S.G. (1990) El Niño, La Niña and the Southern Oscillation. Academic Press, London, 293 p.
- [9] Jury, M.R. and Pathack, B.M.R. (1991) A Study of Climate and Weather Variability over the Tropical Southwest Indian Ocean. *Meteorology and Atmospheric Physics*, **47**, 37-48. <https://doi.org/10.1007/BF01025825>
- [10] Jury, M.R. and Pathack, B.M.R. (1993) Composite Climatic Patterns Associated with Extreme Modes of Summer Rainfall over Southern Africa: 1975-1984. *Theoretical and Applied Climatology*, **47**, 137-145. <https://doi.org/10.1007/BF00867446>
- [11] Landman, W.A. (1995) A Canonical Correlation Analysis Model to Predict South African Summer Rainfall. *Experimental Long-Lead Forecast Bulletin*, **4**, 23-24.
- [12] Jury, M.R., Pathack, B.M.R., Rautenbach, C.J.W. and Van Heerden, J. (1996) Drought over South Africa and Indian Ocean SSTs: Statistical and GCM Results. *The Global Atmosphere and Ocean System*, **4**, 47-63.
- [13] Tennant, W.J. (1996) Influence of Indian Ocean Sea-Surface Temperature Anomalies on the General Circulation of Southern Africa. *South African Journal of Science*, **92**, 289-295.
- [14] Landman, W.A. and Klopper, E. (1998) 15-Year Simulation of December to March Rainfall Season of the 1980s and 1990s Using Canonical Correlation Analysis (CCA). *Water SA*, **24**, 281-285.
- [15] Rautenbach, C.J.W. (1998) The Unusual Rainfall and Sea Surface Temperature Characteristics in the South African Region during the 1995/96 Summer Season. *Water SA*, **24**, 165-172.
- [16] Cai, W., Wu, L., Lengaigne, M., Li, T., McGregor, S., Kug, J.-S., Yu, J.-Y., *et al.* (2019) Pantropical Climate Interactions. *Science*, **363**, eaav4236.
<https://doi.org/10.1126/science.aav4236>
- [17] Bertrand, A., Lengaigne, M., Takahashi, K., Avadí, A., Poulain, F. and Harrod, C. (2020) El Niño Southern Oscillation (ENSO) Effects on Fisheries and Aquaculture. FAO Fisheries and Aquaculture. Technical Paper No. 660, FAO, Rome.
- [18] Monerie, P.A., Robson, J., Dong, B., Dieppois, B., Pohl, B. and Dunstone, N. (2019) Predicting the Seasonal Evolution of Southern African Summer Precipitation in the DePreSys3 Prediction System. *Climate Dynamics*, **52**, 6491-6510.
<https://doi.org/10.1007/s00382-018-4526-3>
- [19] Hoell, A., Funk, C., Magadzire, T., Zinke, J. and Husak, G. (2015) El Niño-Southern Oscillation Diversity and Southern Africa Teleconnections during Austral Summer. *Climate Dynamics*, **45**, 1583-1599. <https://doi.org/10.1007/s00382-014-2414-z>
- [20] Hoell, A., Funk, C., Zinke, J. and Harrison, L. (2017) Modulation of the Southern Africa Precipitation Response to the El Niño Southern Oscillation by the Subtropical Indian Ocean Dipole. *Climate Dynamics*, **48**, 2529-2540.
<https://doi.org/10.1007/s00382-016-3220-6>
- [21] Archer, E.R.M., Landman, W.A., Tadross, M.A., Malherbe, J., Weepener, H., Maluleke, P. and Marumbwa, F.M. (2017) Understanding the Evolution of the 2014-2016 Summer Rainfall Seasons in Southern Africa: Key Lessons. *Climate Risk Management*, **16**, 22-28. <https://doi.org/10.1016/j.crm.2017.03.006>

- [22] Winsemius, H., Dutra, E., Engelbrecht, F., Archer van Garderen, E., Wetterhall, F., Pappenberger, F. and Werner, M. (2014) The Potential Value of Seasonal Forecasts in a Changing Climate in Southern Africa. *Hydrology and Earth System Sciences*, **18**, 1525-1538. <https://doi.org/10.5194/hess-18-1525-2014>
- [23] Alemaw, B.F. and Chaoka, T.R. (2006) The 1950-1998 Warm ENSO Events and Regional Implications to River Flow Variability in Southern Africa. *Water SA*, **32**, 459-463. <https://doi.org/10.4314/wsa.v32i4.5153>
- [24] Yeh, S.W., Cai, W., Min, S.-K., McPhaden, M.J., Dommengot, D., Dewitte, B. and Collins, M. (2018) ENSO Atmospheric Teleconnections and Their Response to Greenhouse Gas Forcing. *Reviews of Geophysics*, **56**, 185-206. <https://doi.org/10.1002/2017RG000568>
- [25] Amarasekera, K.N., Lee, R.F., Williams, E.R. and Eltahir, E.A.B. (1997) ENSO and the Natural Variability in the Flow of Tropical Rivers. *Journal of Hydrology*, **200**, 24-39. [https://doi.org/10.1016/S0022-1694\(96\)03340-9](https://doi.org/10.1016/S0022-1694(96)03340-9)
- [26] Chen, D., Zebiak, S.E., Busalacchi, A.J. and Cane, M.A. (1995) An Improved Procedure for El Niño Forecasting: Implications for Predictability. *Science*, **269**, 1699-1702. <https://doi.org/10.1126/science.269.5231.1699>
- [27] Taylor, K.E., Stouffer, R.J. and Meehl, G.A. (2012) An Overview of CMIP5 and the Experiment Design. *Bulletin of the American Meteorological Society*, **93**, 485-498. <https://doi.org/10.1175/BAMS-D-11-00094.1>
- [28] Ziese, M., Becker, A., Finger, P., Meyer-Christoffer, A., Rudolf, B. and Schneider, U. (2011) GPCC First Guess Product at 1.0°: Near Real-Time First Guess Monthly Land-Surface Precipitation from Rain-Gauges Based on SYNOP Data.
- [29] Huffman, G.J., Adler, R.F., Rudolf, B., Schneider, U. and Keehn, P.R. (1995) Global Precipitation Estimates Based on a Technique for Combining Satellite-Based Estimates, Rain Gauge Analysis, and NWP Model Precipitation Information. *Journal of Climate*, **8**, 1285-1295. [https://doi.org/10.1175/1520-0442\(1995\)008<1284:GPEBOA>2.0.CO;2](https://doi.org/10.1175/1520-0442(1995)008<1284:GPEBOA>2.0.CO;2)
- [30] Xie, P. and Arkin, P.A. (1997) Global Precipitation 17-Year Monthly Analysis Based on Gauge Observations, Satellite Estimates, and Numerical Model Outputs. *Bulletin of the American Meteorological Society*, **78**, 2539-2558. [https://doi.org/10.1175/1520-0477\(1997\)078<2539:GPAYMA>2.0.CO;2](https://doi.org/10.1175/1520-0477(1997)078<2539:GPAYMA>2.0.CO;2)
- [31] SA FRIEND Database (2020) Southern Africa Flow Database of SA FRIEND. https://www.bafg.de/GRDC/EN/04_spcldtbss/45_SAFL/SA%20_Flow.html
- [32] NOAA (2021) Southern Oscillation Index (SOI). National Ventres for Environmental Information. <https://www.ncdc.noaa.gov/teleconnections/enso/indicators/soi>
- [33] Hirsch, R.M., Helsel, D.R., Cohn, T.A. and Gilroy, E.J. (1993) Statistical Analysis of Hydrologic Data. In: Maidment, D.R., Ed., *Handbook of Hydrology*, McGraw-Hill, London, 17.1-17.55.
- [34] Press, W.H., Flannery, B.P., Teukolsky, S.A. and Vetterling, W.T. (1992) Numerical Recipes: The Art of Scientific Computing. Cambridge University Press, New York, 973.
- [35] Pascale, S., Pohl, B., Kapnick, S.B. and Zhang, H. (2019) On the Angola Low Interannual Variability and Its Role in Modulating ENSO Effects in Southern Africa. *Journal of Climate*, **32**, 4783-4803. <https://doi.org/10.1175/JCLI-D-18-0745.1>
- [36] Nicholson, S.E. and Kim, J. (1997) The Relationship of the El Niño-Southern Oscillation to African Rainfall. *International Journal of Climatology*, **17**, 117-135. [https://doi.org/10.1002/\(SICI\)1097-0088\(199702\)17:2<117::AID-JOC84>3.0.CO;2-O](https://doi.org/10.1002/(SICI)1097-0088(199702)17:2<117::AID-JOC84>3.0.CO;2-O)

-
- [37] FEWSnet (2020) Famine Early Warning Systems Network, Southern Africa Food Security Alert. 2. <https://fewsn.net/southern-africa>
- [38] Hoell, A. and Cheng, L. (2018) Austral Summer Southern Africa Precipitation Extremes Forced by the El Niño Southern Oscillation and the Subtropical Indian Ocean Dipole. *Climate Dynamics*, **50**, 3219-3236. <https://doi.org/10.1007/s00382-017-3801-z>
- [39] Reason, C.J.C. and Smart, S. (2015) Tropical Southeast Atlantic Warm Events and Associated Rainfall Anomalies over Southern Africa. *Frontiers in Environmental Science*, **3**, 1-11. <https://doi.org/10.3389/fenvs.2015.00024>
- [40] Reason, C.J.C. (1998) Warm and Cold Events in the Southeast Atlantic/Southwest Indian Ocean Region and Potential Impacts on Circulation and Rainfall over Southern Africa. *Meteorology and Atmospheric Physics*, **69**, 49-65. <https://doi.org/10.1007/BF01025183>
- [41] Reason, C.J.C. (2001) Subtropical Indian Ocean SST Dipole Events and Southern African Rainfall. *Geophysical Research Letters*, **28**, 2225-2227. <https://doi.org/10.1029/2000GL012735>
- [42] Morioka, Y., Engelbrecht, F. and Behera, S. (2015) Potential Sources of Multidecadal Climate Variability over Southern Africa. *Journal of Climate*, **28**, 8695-8709. <https://doi.org/10.1175/JCLI-D-15-0201.1>
- [43] Meehl, G.A., Goddard, L., Murphy, J., *et al.* (2009) Decadal Prediction. *Bulletin of the American Meteorological Society*, **90**, 1467-1485. <https://doi.org/10.1175/2009BAMS2778.1>
- [44] SADC (2019) The 2019 Synthesis Report on the State of Food and Nutrition Security and Vulnerability in Southern Africa. SADC Secretariat. 22.
- [45] Janowiak, J.E. and Xie, P. (1999) CAMS-OPI: A Global Satellite-Rain Gauge Merged Product for Real-Time Precipitation Monitoring Applications. *Journal of Climate*, **12**, 3335-3342. [https://doi.org/10.1175/1520-0442\(1999\)012<3335:COAGSR>2.0.CO;2](https://doi.org/10.1175/1520-0442(1999)012<3335:COAGSR>2.0.CO;2)